Heterogeneity of Rift Valley fever virus transmission potential across livestock hosts, quantified through a model-based analysis of host viral load and vector infection

Hélène Cecilia[1]*, Roosmarie Vriens[2], Jeroen Kortekaas[3,4],

Paul J. Wichgers Schreur[3], Mariken de Wit[2], Raphaëlle Métras[5],

Pauline Ezanno[1], Quirine A. ten Bosch[2]*

[1] INRAE, Oniris, BIOEPAR, 44300, Nantes, France

[2] Quantitative Veterinary Epidemiology, Wageningen University and Research, Wageningen, The Netherlands

[3] Wageningen Bioveterinary Research, Lelystad, The Netherlands

[4] Laboratory of Virology, Wageningen University & Research, Wageningen, The Netherlands

[5] Sorbonne Université, INSERM, Institut Pierre Louis d'Epidémiologie et de Santé Publique (IPLESP), F-75012, Paris, France

* corresponding authors

Abstract

Rift Valley fever (RVF) is a viral, vector-borne, zoonotic disease. The relative contributions of livestock species to RVFV transmission has not been previously quantified. To estimate their potential to transmit the virus over the course of their infection, we 1) fitted a within-host model to viral RNA and infectious virus measures, obtained daily from infected lambs, calves, and young goats, 2) estimated the relationship between vertebrate host infectious titers and probability to infect mosquitoes, and 3) estimated the net infectiousness of each host species over the duration of their infectious periods, taking into account different survival outcomes for lambs. Our results indicate that the efficiency of viral replication, along with the lifespan of infectious particles, could be sources of heterogeneity between hosts. For similar infectious titers, we found that infection rates in *Aedes* spp. vectors were significantly higher than in *Culex* spp. vectors. Consequently, for *Aedes* infections, we estimated the net infectiousness of lambs to be 2.93 (median) and 3.65 times higher than that of calves and goats, respectively. Among lambs, individuals which eventually died from the infection were 1.93 times more infectious than lambs recovering. Beyond infectiousness, the relative contributions of host species to transmission depend on local ecological factors, including relative abundances and vector host-feeding preferences. Quantifying these contributions will ultimately help design

efficient, targeted, surveillance and vaccination strategies.

1 Introduction

At the beginning of this century, 75% of emerging pathogens in humans were estimated to be zoonotic (Taylor et al., 2001) and 77% of livestock pathogens could be transmitted between different host species (Cleaveland et al., 2001). Estimating the relative role different species play in sustaining or amplifying pathogen spread is fundamental for designing control strategies (Hollingsworth et al., 2015; Buhnerkempe et al., 2015; Lloyd-Smith et al., 2015; Webster et al., 2017), yet is hampered by an incomplete understanding of the host(-vector)-pathogen interactions that underlie the spread of these pathogens (Roche et al., 2013; Vazquez-Prokopec et al., 2016; Fenton et al., 2015; Martin et al., 2019).

The potential of a host to contribute to virus transmission is determined by the complex interplay of different factors. For viruses transmitted by arthropod vectors (i.e., arboviruses) these epidemiological interactions are driven both by ecological, population-level factors (i.e., the presence of specific host and vector species and their respective interactions) and the individual-level interactions of the virus with its hosts and vectors. The ability of a host species to infect a susceptible vector upon a potentially infectious contact is determined by the latter. Namely, it derives from i) the viral replication in the host and ii) the ability of a vector to pick up the virus upon blood feeding and subsequently become infected and infectious. While these processes can and have been studied in experimental settings, combining these findings into epidemiologically meaningful parameters is challenging (Althouse and Hanley, 2015; Bosch et al., 2018; Kain and Bolker, 2019).

Within-host mathematical models and accompanying inference frameworks have been developed to aid the analysis and interpretation of viral load patterns obtained in controlled infection experiments. Such models provide insights into the biological mechanisms underlying observed patterns (Clapham et al., 2014; Ben-Shachar and Koelle, 2015; Ben-Shachar et al., 2016; Clapham et al., 2016; Koelle et al., 2019) and how those patterns relate to the clinical expression of the disease (Bosch et al., 2018). The majority of these modelling efforts are based on viral RNA (or DNA) data, which are indirect measures of infectious virus. Efforts to combine these with infectious virus data (e.g., median tissue culture infectious dose, $TCID_{50}$ or plaque forming units, PFU) have recently emerged for influenza viruses and provide better mechanistic insights into the proportion of particles that are infectious and could contribute to onward transmission (Schulze-Horsel et al., 2009; Pinilla et al., 2012; Petrie et al., 2013, 2015; Simon et al., 2016; Yan et al., 2020).

Rift Valley fever virus (RVFV) exemplifies the challenges inherent to battling multi-host arboviruses. It was first identified in Kenya, in 1930, after description of an enzootic hepatitis in sheep (Daubney et al., 1931). The

virus has since caused outbreaks throughout the African continent as well as in the Southwest Indian ocean islands (Comoros archipelago, Madagascar) and the Arabian Peninsula (Nanyingi et al., 2015). RVFV mainly affects sheep, goats, and cattle, in which it causes abortion storms and sudden death of newborns (Al-Afaleq and Hussein, 2011; El Mamy et al., 2011). Spillover to humans happens through the handling of infectious animal tissue or by vectorial transmission. While most human infections remain asymptomatic or manifest as a mild illness, symptoms can range from flu-like to hepatitis, retinitis and in the most severe cases, haemorrhagic disease (LaBeaud et al., 2010). RVFV vector-borne transmission is mainly mediated by *Aedes* and *Culex* spp. mosquitoes, making its establishment possible in a wide range of ecosystems (Linthicum et al., 2016). While sheep are generally believed to be the most important host species (Bird et al., 2009; Clark et al., 2018; Bron et al., 2021), efforts fall short of quantifying livestock hosts relative contribution to RVFV transmission.

Here, we aim to gain more insight into the relative importance of livestock species in RVFV transmission. Using experimental data and mathematical modeling, we derive estimates of hosts' individual potential to transmit RVFV to vectors during their infection.

2 Results

2.1 Overall approach

We developed a mechanistic compartmental within-host model, representing the infection of target cells and the subsequent production of viral particles, not all of which are infectious (Figure 1). We distinguish the total amount of viral particles produced by infected cells, V_{tot}, and the subpart capable of infecting new cells, V_{inf}. We fitted this model to time-series of viral RNA (RT-qPCR) and infectious virus (TCID$_{50}$), measured in experimentally infected calves, lambs, and young goats. We compared the cell-level basic reproduction number R_0 and mean generation time T_g, between groups. We quantified the relationship between vertebrate hosts' infectious titers and transmission to mosquitoes using data extracted from a literature review. Finally, we estimated the net infectiousness of livestock species, a metric proportional to the number of mosquitoes a host would infect over the entire course of its infection.

2.2 Data

Data on viral RNA and infectious virus were obtained from a published study on a candidate RVFV vaccine (Wichgers Schreur et al., 2020a) (Section 4). Mock vaccinated animals were infected with a virulent RVFV strain. Eight animals were exposed per species (lambs, calves, young goats), all animals became viraemic. An additional dataset obtained from 8 lambs, following the same protocol, was added. In total, 10/16 lambs succumbed to the infection or were euthanized, 3 to 7 days after RVFV inoculation, while others survived until the end of the experiment (2 weeks). All calves and young goats survived until the end of the experiment.
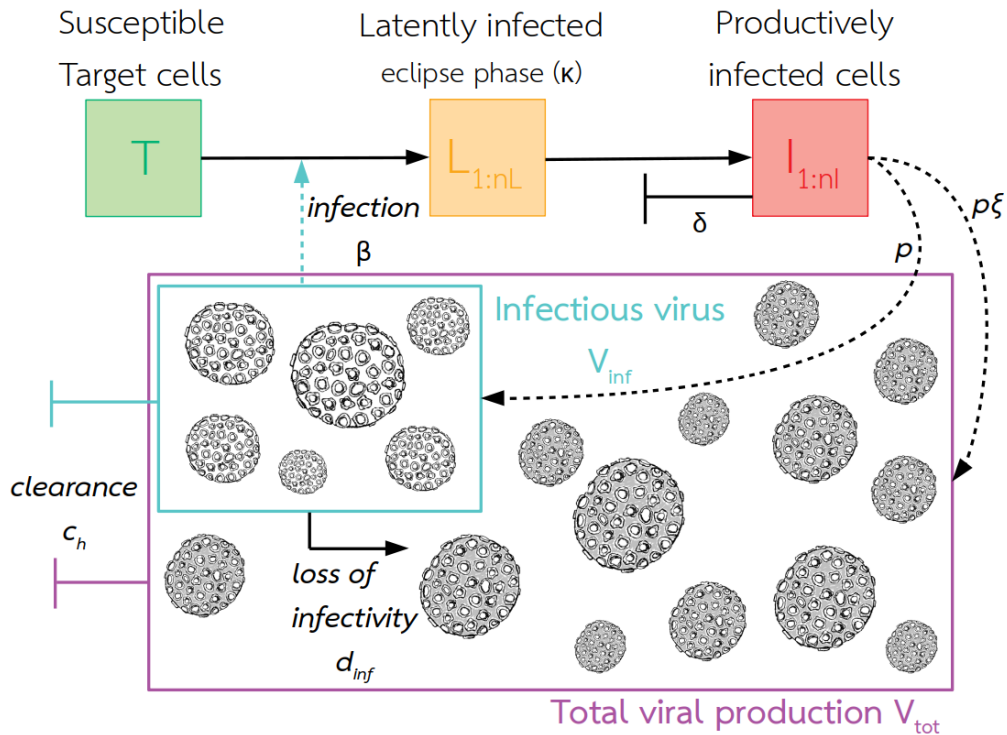
Figure 1: Graphical representation of the within-host model. Infectious viruses V_{inf} were fitted to $TCID_{50}$ measures, and total viral production V_{tot} to RT-qPCR measures. The eclipse phase (state L) is the period between the infection of a cell by a virus and the appearance of mature virus within the cell. Productively infected cells I are the only ones producing progeny virions. Subscripts in L and I indicate the use of Erlang distributions for the time spent in those states. Target cells are not replenished and only productively infected cells die. Model assumptions, equations and parameter definitions can be found in Section 4, Eq. 1, and Table 2.

2.3 Within-host model of RVFV infection

We fitted a within-host model to four datasets, measuring viral RNA and infectious virus in RVFV-infected lambs (surviving ; dying), calves, and young goats, using a Bayesian framework (Section 4). The model consisted of 10 parameters, 5 of which were held constant (Table 2). We estimated the death rate δ of infected cells, their total daily production of viral particles ξp, among which p are infectious, the degradation rate d_{inf} of infectious viruses into non-infectious viruses, and the clearance rate c_h of viral particles. Parameter values were then used to calculate the cell-level basic reproduction number R_0 and mean generation time T_g. Initial conditions were set using elements of the experimental protocol along with a sensitivity analysis (Section 4, Table 2). Outputs from the Markov Chain Monte Carlo (MCMC) procedure can be found in Supplementary Information S.1. The fits satisfyingly capture the dynamics present in the data (Figure 2).

The model selection performed highlights different viral load dynamics between livestock species (Deviance Information Criterion (DIC) 1307 *vs* 1186, comparison based on surviving animals as calves and young goats all survived, Figure 2). In particular, the ratio of daily viral RNA over infectious viruses produced (ξ) is the highest in the goat group, meaning that the replication process might be less efficient in this species (Table 1). The

highest density intervals (HDIs) for this parameter are wide (Table 1), but the posterior distributions remain informative (Figure S.4). In addition, among surviving hosts, the lifespan of infectious particles $(d_{inf} + c_h)^{-1}$ is estimated to be the longest in goats (Table 1). The resulting dynamics show viremia in goats peaks sooner than in calves and in lambs, but with a lower peak value for infectious viruses (Figure 2). Lambs have on average the most infectious viral particles. Model results indicate this could be a result of a slightly higher daily production rate p (Table 1), as well as their initial susceptible cell population, which we estimated to be higher than in other species (Figure S.1). Characterizing the infectious replication process through the basic reproduction number R_0 and generation time T_g (Section 4, Eq. 2-3) shows no strong differences between species when comparing surviving individuals (Figure 3). R_0 ranges from 8.51 (median; 95% HDI 5.69 - 14.53) for calves, to 11.47 (median; 95% HDI 7.73 - 17.68) for lambs. T_g (i.e., the time between infection of a cell and infection of a secondary cell) ranges from 13.48h (median; 95% HDI 12.84h - 15.23h) in goats to 14.43h (median; 95% HDI 12.82h - 18.31h) in calves.

Among lambs, individuals succumbing to RVF are characterized by higher viral loads, both total and infectious, and a slower decay after the peak is reached (Figure 2). The best model fit is achieved when allowing parameters to vary depending on the survival of the individuals (Figure 2, DIC 928 vs 745), indicating significantly different within-host dynamics depending on clinical outcome. In particular, we estimated that both infected cells and infectious viral particles have prolonged lifespans in dying lambs (δ^{-1} and $(d_{inf} + c_h)^{-1}$ respectively, Table 1). This impacts R_0 which is 1.88 times higher (median ratio; 95% HDI 0.84 ; 3.51) in dying individuals than surviving ones, and T_g, which is 1.19 times longer (median ratio; 95% HDI 0.91 ; 1.65) in dying individuals than surviving ones. Besides, the ratio of daily viral RNA over infectious viruses produced (ξ), which does not influence R_0, is higher in dying lambs than surviving ones (Table 1).
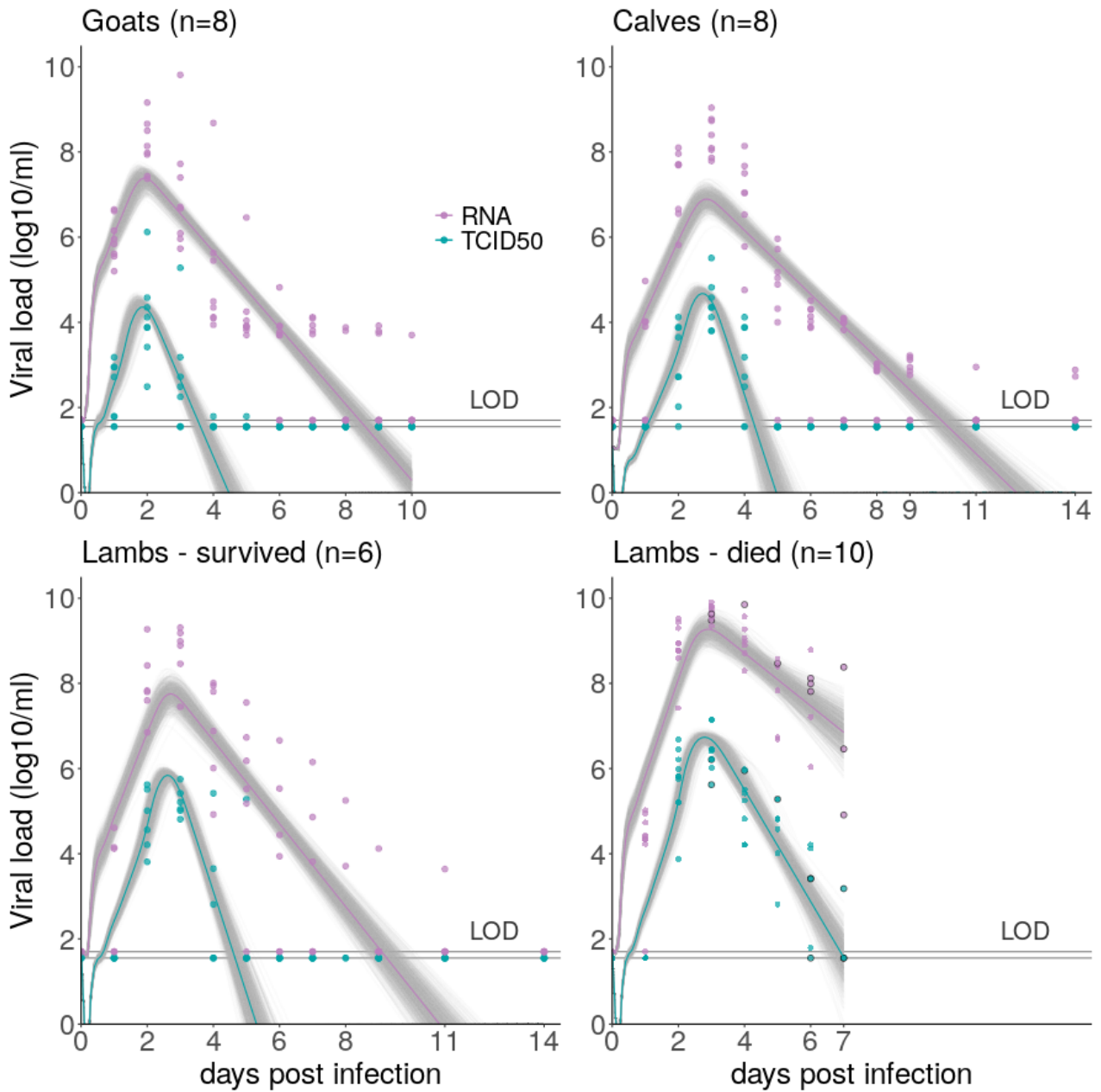
Figure 2: Data on viral RNA (RT-qPCR) and infectious virus (TCID$_{50}$), in log$_{10}$/ml of plasma, and model fits, for host groups showing significantly different viral dynamics. Circles are data points. Solid colored lines show predicted median. Grey lines represent model trajectories resulting from 1000 parameter sets sampled in posterior distributions. Purple is for viral RNA and blue for infectious viruses. For lambs which died from RVF, circled points represent individuals' time of death. LOD = limit of detection, 1.55 for TCID$_{50}$, 1.7 for viral RNA (log$_{10}$)

		Estimate : median [HDI]			
	Parameter	Goat	Calf	Lamb surv.	Lamb dead
δ	I death rate	2.61 [1.91 ; 3.0]	2.17 [1.30 ; 3.0]	2.34 [1.60 ; 3.0]	1.52 [0.85 ; 2.44]
p	production of V_{inf}	20.14 [13.33 ; 29.40]	14.98 [12.31 ; 17.89]	21.53 [17.09 ; 26.50]	25.27 [19.72 ; 31.00]
ξ	ratio $\frac{V_{tot}}{V_{inf}}$ produced	672.76 [333.96 ; 999.56]	75.16 [20.60 ; 161.05]	44.33 [9.66 ; 104.48]	221.15 [50.57 ; 510.97]
d_{inf}	degradation $V_{inf} \rightarrow V_{tot}$	2.10 [1.36 ; 2.92]	3.77 [2.17 ; 6.63]	3.26 [2.19 ; 4.48]	1.60 [0.90 ; 2.31]
c_h	clearance of V_{inf} and V_{tot}	2.06 [1.88 ; 2.24]	1.72 [1.53 ; 1.92]	2.24 [1.94 ; 2.53]	1.43 [0.87 ; 2.01]

Table 1: Parameter estimates per host group. Median of joint posterior distributions (3 chains) and HDI = highest density interval (95%). All parameters are in unit day^{-1}, see Section 4 for detailed definitions. The HDI is built such as every point inside the interval has higher credibility than any point outside the interval (Kruschke, 2015).
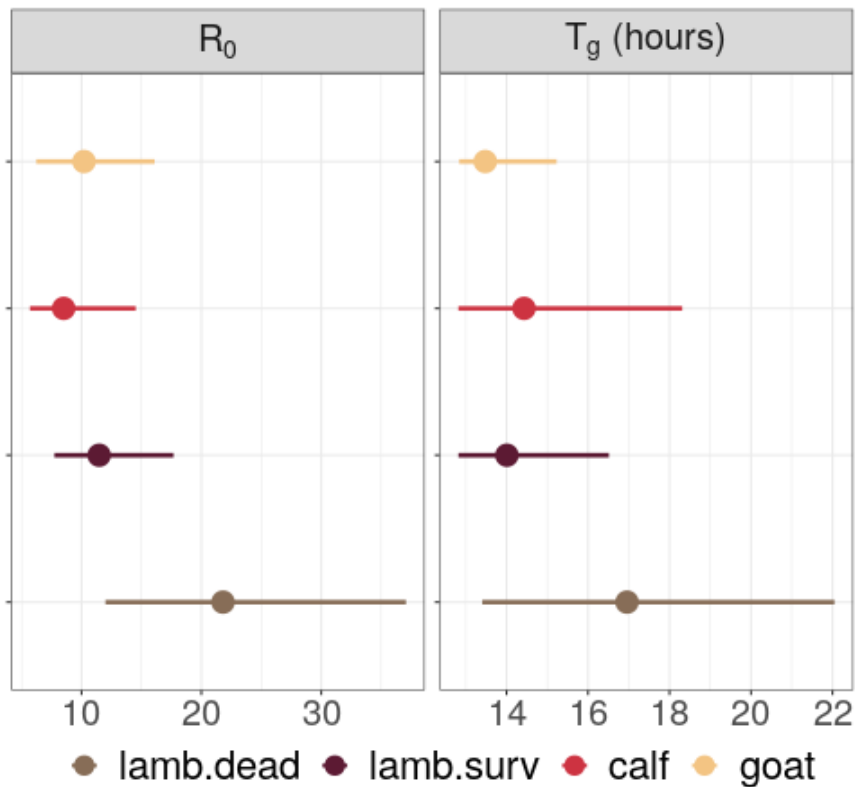

Figure 3: Outcome measures per host group. Points are median estimates, lines show highest density intervals, computed from joint posterior distributions (3 chains). Basic reproduction number R_0 is computed with Eq. 2 and generation time T_g with Eq. 3. Note that generation times are constrained in their lower values due to the eclipse phase duration (κ^{-1}) and rate of virus entry into cells (β) being fixed (Table 2).

2.4   Dose-response relationship in RVFV mosquito vectors

Through a systematic review, we identified 9 papers from which data could be extracted to estimate the relationship between vertebrate host infectious titers and associated infection rates in vectors (Section 4, Supplementary Information S.2.1). Selected experiments were performed with hamster hosts, *Aedes* or *Culex* spp. vectors, using RVFV strain ZH501.

Dose-response curves differ significantly between *Aedes* and *Culex* spp. (Figure 4, Supplementary Information S.2). At 5 $\log_{10}$ TCID$_{50}$/ml for instance, which most animals could reach or exceed (Figure 2), there is 25% [15 ; 38] probability to infect an *Aedes* spp. vector and 11% [7 ; 18] probability to infect a *Culex* spp. vector (Figure 4). We did not find a significant effect of temperature and number of days post exposure on infection rates (Supplementary Information S.2.2, S.2.3). The effect of dose is best captured by Eq. S.6, used by Ferguson et al., 2015, fitted with a betabinomial likelihood accounting for overdispersal in the data (Supplementary Information S.2.3). Species-specific curves were estimated for *Aedes vexans*, *Aedes japonicus*, *Culex nigripalpus*, and *Culex tarsalis* (Supplementary Information S.2.3, Figure S.6). While there is intra-genus variability, infection rates in *Aedes vexans* and *Aedes japonicus* are on average higher than in *Culex nigripalpus*, and *Culex tarsalis* at similar host infectious titers (Figure S.6).

2.5   Net infectiousness of RVFV livestock hosts

Net infectiousness (NI, Eq. 4) varies with both host species and mosquito genus involved (Section 4, Figure 5). NI is lowest for goats and highest for lambs. The relative differences in NI between host species is stronger when comparing transmission to *Culex* (median ratio lamb:goat 4.79 ; median ratio lamb:calf 3.75) than to *Aedes* mosquitoes (median ratio lamb:goat 3.65 ; median ratio lamb:calf 2.93). Every host type studied has the highest NI when bitten by an *Aedes* spp. vector, but the uncertainty around NI estimates decreases when considering *Culex* bites (Figure 5).
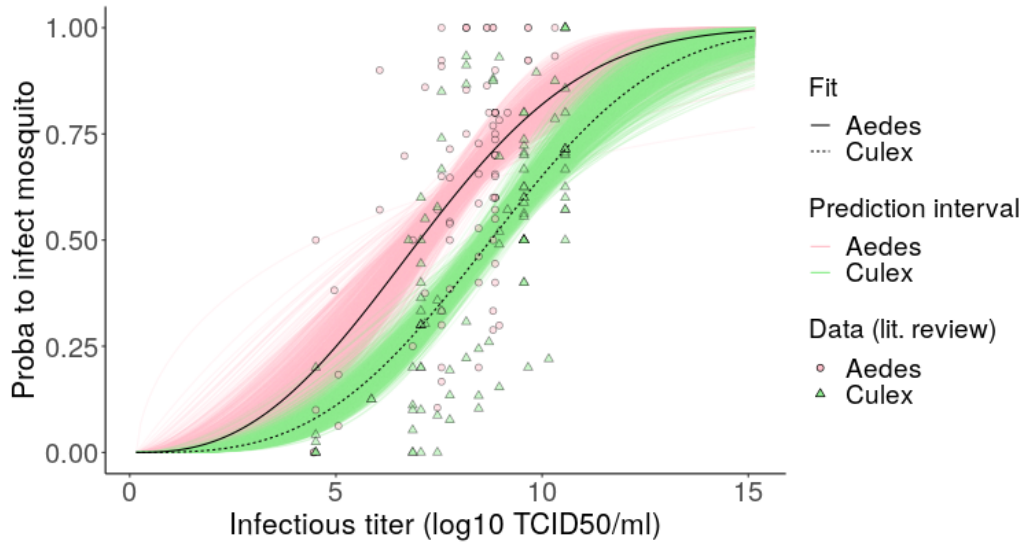
Figure 4: Dose-response relationships linking host infectious titers to the probability to infect mosquito vectors. Data retrieved from a systematic review (Section 4, Supplementary Information S.2). Points and triangles show infection rates (presence of RVFV in mosquito bodies, legs excluded) from experiments performed with hamsters with RVFV strain ZH501. Fits were obtained with Eq. S.6 using a betabinomial likelihood to account for overdispersion in the data. Prediction intervals correspond to trajectories resulting from 1000 parameter sets sampled in posterior distributions. Note that infectious titers >10 $\log_{10}$ are not to be expected in hosts, but were included to show the full curve.
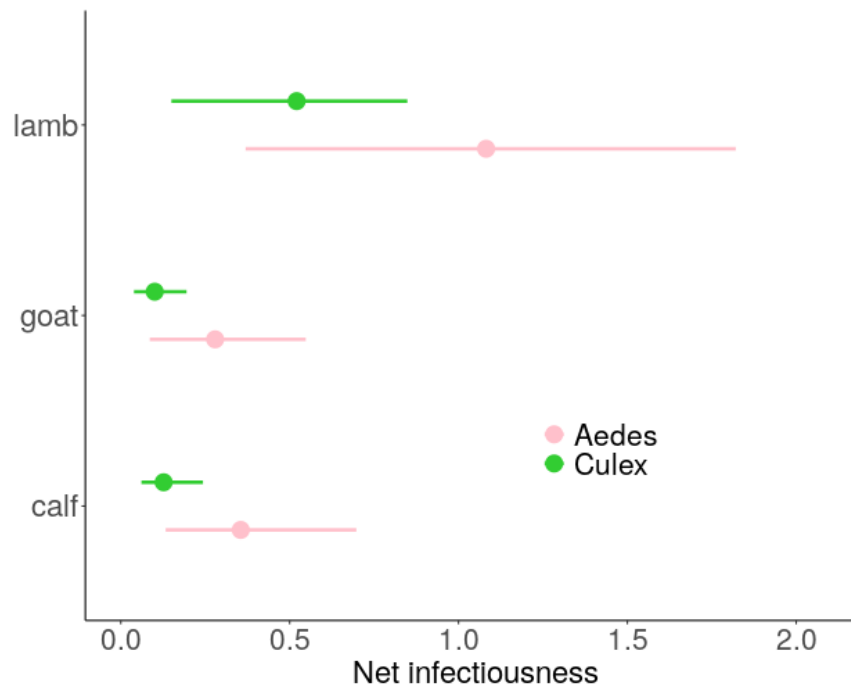

Figure 5: Net infectiousness of RVFV livestock host species, function of the mosquito genus involved in transmission. Points are median estimates, lines show highest density intervals, computed using 1000 parameter sets sampled in joint posterior distributions (3 chains). For lambs, parameters were sampled in the posteriors of both surviving and dying groups, according to the survival rate observed in the original dataset (6/16, Figure S.7). Time of death also varied according to a Weibull survival model (Section 4).

Lambs' NI varies with the expected death rate among lambs (Section 4, Figure S.7). Lambs dying from RVF have a higher NI than lambs surviving (Figure S.7). Indeed, dying lambs are more infectious than their surviving

9

counterparts during their whole viremic period, which in 60% of cases can last longer (day 7) than the infectious period of surviving individuals (probability $< 1\%$ to infect an *Aedes* or a *Culex* past day 5 post inoculation). When bitten by an *Aedes* spp. vector, lambs NI ranges from 0.24 to 2.54, increasing by a factor 1.93 (median ratio) from surviving to succumbing individuals. When bitten by a *Culex* spp. vector, lambs NI ranges from 0.12 to 1.36, increasing by a factor 2.22 (median ratio) from surviving to succumbing individuals.

3   Discussion

We have presented the results of a data-driven estimation of livestock hosts RVFV transmission potential, providing mechanistic insights into potential sources of heterogeneity between species. Our results demonstrate that sheep are the most infectious livestock hosts, and that virulent infection leading to death reinforces the infectiousness of this species. We also showed that lower infectious doses are needed to infect *Aedes* spp. vectors than *Culex* spp.. The framework presented here can be applied to other multi-host arboviruses to estimate transmission potential, a key component of hosts contribution to transmission at large scale.

The suite of experimental data used in our study incorporated the major elements needed for an epidemiologically relevant estimation of hosts transmission potential. We included both viral RNA and infectious viruses, measured *in vivo*, in natural RVFV hosts. Similar existing models used data coming either from *in vitro* experiments (Schulze-Horsel et al., 2009; Iwami et al., 2012; Pinilla et al., 2012; Simon et al., 2016; Yan et al., 2020), or from model hosts, such as ferrets for influenza (Petrie et al., 2013, 2015). The breeds infected in our dataset make our estimates directly relevant for scenarios of RVFV emergence in Europe, and a comparison with African breeds would be an appropriate next step, along with the comparison of several RVFV strains (Vloet et al., 2017; Fontaine et al., 2018). Performing infection through mosquito bites rather than intravenous injection would ensure a natural course of infection, although the protocol presently used was shown to yield similar viral load dynamics as mosquito-mediated infection (Wichgers Schreur et al., 2021). This would further allow for the exploration of the impact of heterogeneity of exposure (i.e., number of infectious bites or infectious titers in vector saliva) on infectiousness. Finally, data on adult livestock as well as human viremia levels will be key to complete our understanding of hosts contribution to RVFV transmission.

Our within-host model is the second developed for RVFV (Tuncer et al., 2016), but the first to mechanistically represent the process of viral production from host cells. This enabled an identification of processes driving differences between groups and an increased understanding of the cell-level viral replication process. First, we estimated a less efficient replication in goats, further advocating for the use of infectious virus measures in order not to overestimate transmission potential (Tesla et al., 2018). Besides, we estimated the lifetime of infectious viral particles and infected cells to be longer in dying lambs than their surviving counterparts, which calls for an

exploration of corresponding (immune) mechanisms in future experiments. The uncertainty around parameter estimates remains important, and summarizing parameter estimates into aggregated outcome measures R_0 and T_g put those mechanistic differences into perspective. Indeed, once correlation between parameters are taken into account, the replication process is most different between severe and moderate infection within sheep and less so between host species. The model could be refined by incorporating an explicit immune response (Elliott and Weber, 2009; Mapder et al., 2019) or taking into account the genomic composition of viral particles (Jacobs et al., 2019; Bermúdez-Méndez et al., 2021), but the quantity of information needed (number of timesteps and replicates, inclusion of data on immune responses) could hamper this costly data collection.

By gathering relevant competence studies into a meta-analysis, we quantified the relationship between infectious titers and mosquito RVFV infections. To our knowledge, such dose-response relationship had not been quantified for RVFV. This results in a lack of precision in between-host RVFV transmission models which usually assume constant infectiousness of hosts over their infectious period. Quantifying how the probability to infect a vector increases with dose will also affect the stochasticity of transmission in small populations (be it emergence or extinction). Dose-response curves have been important for the study of other arboviruses, e.g., for exploring the role of asymptomatic dengue infections (Bosch et al., 2018) or the epidemic potential of *Aedes albopictus* for Zika virus (Lequime et al., 2020). One important originality of our work was to highlight a higher susceptibility of *Aedes* spp. vectors to RVFV infection compared to *Culex* spp. vectors, at similar infectious titers. Further studies are needed to confirm whether this higher probability of infection is also accompanied by a higher probability of the mosquito becoming infectious itself. This would require the detection of infectious particles in mosquitoes' saliva, which was only performed in 23 out of 185 data points in the present systematic review.

A lot remains unknown about the bottlenecks of arboviruses propagation in mosquitoes (Weaver et al., 2021). It can depend on species within each genus (Bustamante and Lord, 2010; Golnar et al., 2014) or even mosquito provenance (field *vs* laboratory-reared, Turell et al., 2008, 2010, 2013), in part because of the role of temperature (Turell et al., 2020). Further experiments are needed to know whether a given infectious titer sampled during the increasing or the decreasing phase of viral dynamics would yield the same probability to infect vectors. This comes down to defining what makes a viral particle infectious to host cells *vs* vector cells, and might relate to the efficiency of genome packaging by those cells (Bermúdez-Méndez et al., 2021). Mechanistic modeling will help grasp the complexity of involved processes.

Our study provided key estimates of RVFV livestock hosts' transmission potential. It quantified for the first time the prominent role of sheep, which are 3 to 4 times more infectious than cattle and goats, due to more infectious viruses and a longer infectious period. In addition, fatal infection in sheep does not diminish trans-

mission potential but could rather increase it, based on time of deaths observed in our dataset. This entails that most vulnerable populations, in addition to suffering more deaths, will likely experience larger outbreaks.

Understanding the relationship between infectiousness and pathogen load represents a key challenge to connect modeling scales (Gog et al., 2015). We have importantly contributed to deciphering this relationship for Rift Valley fever virus. Combining these results with ecological factors such as vector presence, population dynamics, and trophic preference, as well as human factors which define the presence of livestock hosts and their mobility, will increase our understanding of RVFV transmission dynamics at large scale. These interacting scales might yield unexpected patterns and reshape the way we design surveillance and control strategies for multi-host arboviruses in general.

4 Materials and Methods

4.1 Data

Animals (16 lambs, 8 calves, 8 young goats) were inoculated intravenously with $5 \log_{10} \text{TCID}_{50}$ of strain rRVFV 35/74. Animals' age was 2-3 weeks for calves, 8-10 weeks for lambs and goats. The average body weight of animals, used further to calibrate the inoculum per ml of plasma, was 45 kg for lambs, 30 kg for goats, and 80 kg for calves. Animals were purchased from conventional Dutch farms, and the breed was Texel cross for sheep, Saanen for goats, and Holstein-Friesian for cattle (Wichgers Schreur et al., 2020b).

4.2 Within-host model of RVFV infection

Our mechanistic model (Figure 1) is formulated as a set of ordinary differential equations, and is similar to existing within-host models developed for influenza (Petrie et al., 2013; Yan et al., 2020):

$$
\begin{aligned}
\frac{dT}{dt} &= -\beta T V_{inf} \\
\frac{dL_1}{dt} &= \beta T V_{inf} - n_L \kappa L_1 \\
\frac{dL_i}{dt} &= n_L \kappa (L_{i-1} - L_i), && i = 2, ..., n_L \\
\frac{dI_1}{dt} &= n_L \kappa L_{n_L} - n_I \delta I_1 \\
\frac{dI_j}{dt} &= n_I \delta (I_{j-1} - I_j), && j = 2, ..., n_I \\
\frac{dV_{inf}}{dt} &= p \sum_{j=1}^{n_I} I_j - d_{inf} V_{inf} - c_h V_{inf} - \sigma \beta T V_{inf} \\
\frac{dV_{tot}}{dt} &= \xi p \sum_{j=1}^{n_I} I_j - c_h V_{tot}
\end{aligned}
\tag{1}
$$

In this model, infectious viruses V_{inf} infect susceptible target cells T at rate β. Infected cells first go through a latent state, L (eclipse phase). Then, they become productively infected cells, I. These cells produce viral particles V_{tot} at rate ξp, not all of which are infectious (V_{inf} produced at rate p). Infectious viruses degrade into non-infectious viruses at rate d_{inf}, which does not impact total viral production V_{tot}. A similar host clearance rate c_h is applied to both non-infectious and infectious particles.

To achieve realistic distributions of time spent in L and I states, we used Erlang distributions. This means that infected cells go through n_L latent stages and n_I infectious stages, where the time spent in each stage is exponentially distributed. We used $n_L = n_I = 20$, sufficient for the resulting latent and infectious periods to be almost normally or lognormally distributed (Krylova and Earn, 2013; Lloyd, 2001). The mean of these Erlang distributions are κ^{-1} and δ^{-1}, and their variance $\dfrac{1}{n_L \kappa^2}$ and $\dfrac{1}{n_I \delta^2}$.

We used a target-cell limited model, meaning that the depletion of target cells is what triggers the viral load peak and subsequent decline. We did not incorporate an explicit immune response. However, as explained by Beauchemin and Handel, 2011, this type of model can be seen as equivalent to assuming a constant effect of the immune response (IR). This IR can act implicitly by limiting the number of cells susceptible to the infection, removing infected cells or viral particles.

We fitted V_{inf} to TCID$_{50}$ measures and V_{tot} to RT-qPCR measures. As TCID$_{50}$ measures the dose needed to induce a cytopathic effect in 50% of the cells, a conversion factor σ is needed to express it as a quantity of infectious viruses, usually measured in plaque forming units (PFUs). Here, we set $\sigma = 0.69$ TCID$_{50}$/ml, consistent with 1 ml virus stock having half the number of (PFUs) as TCID$_{50}$ using Poisson sampling (Canini et al., 2016).

We used a Metropolis Rosenbluth Monte Carlo Markov Chain (MCMC) algorithm to fit our model, implemented in R, using the *odin* package (https://github.com/mrc-ide/odin) to speed up simulations. The composite log-likelihood, applied to $\log_{10}$ measures, was similar to Clapham et al., 2014 (errors normally distributed, limit of detection accounted for). Log-likelihoods for total and infectious viruses were summed, as well as across individuals. The score obtained was used by the algorithm to determine if a parameter set should be accepted. At each iteration, parameters were simultaneously sampled using normal distributions centered around their last accepted value, with a standard deviation specific to each parameter. To obtain acceptance rates between 10% and 45% (the optimal acceptance rate being 23.4% as shown by Roberts et al., 1997) for each parameter, we used a custom function which determines appropriate standard deviations for their sampling. Fixed and estimated parameters can be found in Table 2, chosen in agreement with identifiability analyses of similar models (Miao et al., 2011; Beauchemin and Handel, 2011). Priors represent the probability distribution of possible parameter values, based on prior knowledge. We used uniform distributions, with bounds intended to allow a

wide exploration of parameter values while being biologically realistic.

Our fitting procedure worked as follows : for each dataset to fit, we ran small chains (10,000 iterations, 5,000 burn-in period) fixing T_0 at different values spread across [3;6.5] $\log_{10}$/ml plasma. The best T_0 value was then assessed through maximum log-likelihood profiles (Figure S.1) and kept for longer chains. Three long chains were run (100,000 iterations, 20,000 burn-in) for each dataset. The Gelman Rubin diagnostic test was used to assess common convergence of the chains (Supplementary Information S.1).

To determine whether viral load dynamics $V(t)$ differ between livestock host groups, we ran the inference procedure in two distinct ways : treating these groups as equal (aggregating datasets) or different (fitting done for each dataset separately, Supplementary Information S.1). The resulting joint posterior distributions was used to compute the Deviance Information Criterion (DIC) of these models and select those with the smallest DIC (Supplementary Information S.1). We did not attempt to find differences between individuals of a given group.

To characterize the replication process at the beginning of the infection, we computed two outcome measures from the parameters of our model. The basic reproduction number R_0 (Eq. 2, Beauchemin et al., 2008; Yan et al., 2020) is defined as the average number of new infected cells produced by one infected cell introduced into an entirely susceptible target-cell population. The generation time T_g (Eq. 3, Wallinga and Lipsitch, 2007; Svensson, 2007; Yan et al., 2020) is the average time between the infection of a cell and the infection of a secondary cell, again in an entirely susceptible target cell population. The formula for T_g was adapted to a model using Erlang distributions (for time spent in L and I states). How it changes compared to T_g computed for models with exponential distributions is explained in Supplementary Information S.1.

$$R_0 = \frac{\beta T_0 p}{\delta(c_h + d_{inf} + \sigma \beta T_0)} \tag{2}$$

$$T_g = \frac{1}{\kappa} + \frac{n_I + 1}{2n_I} \cdot \frac{1}{\delta} + \frac{1}{c_h + d_{inf} + \sigma \beta T_0} \tag{3}$$

Name	Meaning	Value/Estimated	Reference/Prior
T_0	initial number of susceptible target cells	Fixed within MCMC, estimated *a priori* through likelihood profiles	see Figure S.1
L_0	initial number of latently infected cells	0	
I_0	initial number of productively infected cells	0	
$V_{inf,0}$	initial number of infectious virions	12.5 for calves, 62.5 for goats, 52.6 for lambs (per ml of plasma, total inoculum per animal being 10^5	References for plasma:body weight ratios Quigley et al., 1998; Courtice, 1943; Coghlan et al., 1977
β	rate governing infection of target cells by infectious virions	set such as $\beta T_0 = 48$ day^{-1}	assumed
n_L, n_I	number of L and I states for the Erlang distributions	20	Krylova and Earn, 2013; Lloyd, 2001
κ^{-1}	eclipse phase duration	1/3 day (8 hours)	P. Wichgers-Schreur personal communication, observed *in vitro*
δ	death rate of productively infected cells	Estimated	[0.1 ; 10]° day^{-1}
p	rate of production of infectious virions	Estimated	[0.2 ; 3.10^4]† day^{-1}
d_{inf}	rate of degradation of infectious virions into non-infectious viral particles	Estimated	[0.1 ; 10] day^{-1}
c_h	host-driven clearance rate	Estimated	[0.1 ; 10] day^{-1}
σ	correction factor to convert from infectious virions to TCID$_{50}$	0.69	Canini et al., 2016
ξ	ratio of total viral particles to infectious virions, as produced by infected cells	Estimated	[1 ; 1000]† day^{-1}

Table 2: Parameters of the within-host model. Values if fixed, prior range (uniform distribution) if estimated.
† : these values were applied for each L (respectively I) states, so a daily rate per L (I) cell (not state) can be obtained by multiplying by n_L (n_I)
° : δ was constrained to be inferior to κ and $(c_h + d_{inf})$, as advised by Smith et al., 2010.

4.3 Dose-response relationship in RVFV mosquito vectors

A systematic review of the literature was performed to study $F(V)$, the relationship between a vertebrate host RVFV infectious titer and the associated probability to infect a mosquito upon its bite (Supplementary Information S.2.1). We limited our quantitative analysis to experiments performed with *Aedes* and *Culex* spp., with strain ZH501, on hamsters (Supplementary Information S.2.1). This corresponded to 185 data points from 9 papers.

To assess the impact of the diversity of protocols from which the data originated, we tested the effect of temperature, and number of days between mosquito feeding and dissection, in addition to dose (infectious titer) on infection rates (presence of RVFV in the body of mosquitoes, legs excluded, Supplementary Information S.2.2, S.2.3). For that we used a logistic function (Eq. S.5), fitted with a binomial and a beta-binomial likelihood, the latter to account for overdispersal in the data (Supplementary Information S.2.3).

We used Akaike Information Criterion (AIC) to compare model fit of different functional forms (Supplementary Information S.2.3). Best fitting functions were then used to explore differences between and within genera (Table S.1, Figure S.6).

4.4 Net infectiousness of RVFV livestock hosts

We define net infectiousness (NI) as the integral of an infectiousness curve over time (Eq. 4)

$$NI_{vect,host} = \int F_{vect}(V_{host}(t))dt \tag{4}$$

NI combines the dose-response relationship in vectors $F_{vect}(V)$ with infectious virus dynamics in hosts $V_{host}(t)$. As such, it must incorporate the uncertainty from both estimations. This was done by sampling 1000 parameter sets in $F_{vect}(V)$ and $V_{host}(t)$ posteriors. For lambs, a draw in a Bernoulli distribution first determined whether the viral load dynamics should be of a surviving or dying type. In the latter case, a time of death was sampled in a Weibull survival model fitted to death times present in our dataset, and determined the end of the viral load curve. Finally, a sensitivity analysis explored how the survival rate in the lamb population impacts the average NI of lambs.

This quantity NI is proportional to the expected number of mosquitoes infected by a host over the entire course of its infection, assuming that biting occurs at a constant rate over this period. By extension, the NI ratio of two host categories is identical to the ratio of the expected number of mosquitoes infected by those two types of hosts, assuming bites to be equally distributed over both species. In the present study, NI was also vector-specific.

5 Acknowledgments

6 Funding

References

Al-Afaleq, A. I. and M. F. Hussein (2011). "The Status of Rift Valley Fever in Animals in Saudi Arabia: A Mini Review". en. In: *Vector-Borne and Zoonotic Diseases* 11.12, pp. 1513–1520. DOI: 10.1089/vbz.2010.0245.

Althouse, B. M. and K. A. Hanley (2015). "The tortoise or the hare? Impacts of within-host dynamics on transmission success of arthropod-borne viruses". en. In: *Philosophical Transactions of the Royal Society B: Biological Sciences* 370.1675, p. 20140299. DOI: 10.1098/rstb.2014.0299.

Beauchemin, C. A. and A. Handel (2011). "A review of mathematical models of influenza A infections within a host or cell culture: lessons learned and challenges ahead". en. In: *BMC Public Health* 11.Suppl 1, S7. DOI: 10.1186/1471-2458-11-S1-S7.

Beauchemin, C. A., J. J. McSharry, G. L. Drusano, J. T. Nguyen, G. T. Went, R. M. Ribeiro, and A. S. Perelson (2008). "Modeling amantadine treatment of influenza A virus in vitro". en. In: *Journal of Theoretical Biology* 254.2, pp. 439–451. DOI: 10.1016/j.jtbi.2008.05.031.

Ben-Shachar, R. and K. Koelle (2015). "Minimal within-host dengue models highlight the specific roles of the immune response in primary and secondary dengue infections". en. In: *Journal of The Royal Society Interface* 12.103, p. 20140886. DOI: 10.1098/rsif.2014.0886.

Ben-Shachar, R., S. Schmidler, and K. Koelle (2016). "Drivers of Inter-individual Variation in Dengue Viral Load Dynamics". en. In: *PLOS Computational Biology* 12.11. Ed. by N. M. Ferguson, e1005194. DOI: 10.1371/journal.pcbi.1005194.

Bermúdez-Méndez, E., E. A. Katrukha, C. M. Spruit, J. Kortekaas, and P. J. Wichgers Schreur (2021). "Visualizing the ribonucleoprotein content of single bunyavirus virions reveals more efficient genome packaging in the arthropod host". en. In: *Commun Biol* 4.1, p. 345. DOI: 10.1038/s42003-021-01821-y.

Bird, B. H., T. G. Ksiazek, S. T. Nichol, and N. J. MacLachlan (2009). "Rift Valley fever virus". en. In: 234.7, p. 11.

Bosch, Q. A. ten et al. (2018). "Contributions from the silent majority dominate dengue virus transmission". en. In: *PLOS Pathogens* 14.5. Ed. by N. M. Ferguson, e1006965. DOI: `10.1371/journal.ppat.1006965`.

Bron, G. M., K. Strimbu, H. Cecilia, A. Lerch, S. Moore, Q. Tran, T. A. Perkins, and Q. A. ten Bosch (2021). "Over 100 years of Rift Valley Fever: a patchwork of data on pathogen spread and spillover". en. In: *Pathogens* 10.708. DOI: `10.3390/pathogens10060708`.

Buhnerkempe, M. G., M. G. Roberts, A. P. Dobson, H. Heesterbeek, P. J. Hudson, and J. O. Lloyd-Smith (2015). "Eight challenges in modelling disease ecology in multi-host, multi-agent systems". en. In: *Epidemics* 10, pp. 26–30. DOI: `10.1016/j.epidem.2014.10.001`.

Bustamante, D. M. and C. C. Lord (2010). "Sources of Error in the Estimation of Mosquito Infection Rates Used to Assess Risk of Arbovirus Transmission". en. In: *American Journal of Tropical Medicine and Hygiene* 82.6, pp. 1172–1184.

Canini, L., M. E. J. Woolhouse, T. R. Maines, and F. Carrat (2016). "Heterogeneous shedding of influenza by human subjects and its implications for epidemiology and control". en. In: *Scientific Reports* 6.1. DOI: `10.1038/srep38749`.

Clapham, H. E., V. Tricou, N. Van Vinh Chau, C. P. Simmons, and N. M. Ferguson (2014). "Within-host viral dynamics of dengue serotype 1 infection". en. In: *Journal of The Royal Society Interface* 11.96, p. 20140094. DOI: `10.1098/rsif.2014.0094`.

Clapham, H. E., T. H. Quyen, D. T. H. Kien, I. Dorigatti, C. P. Simmons, and N. M. Ferguson (2016). "Modelling Virus and Antibody Dynamics during Dengue Virus Infection Suggests a Role for Antibody in Virus Clearance". en. In: *PLOS Computational Biology* 12.5. Ed. by R. Antia, e1004951. DOI: `10.1371/journal.pcbi.1004951`.

Clark, M. H. A., G. M. Warimwe, A. Di Nardo, N. A. Lyons, and S. Gubbins (2018). "Systematic literature review of Rift Valley fever virus seroprevalence in livestock, wildlife and humans in Africa from 1968 to 2016". en. In: *PLOS Neglected Tropical Diseases* 12.7. Ed. by C. M. Barker, e0006627. DOI: `10.1371/journal.pntd.0006627`.

Cleaveland, S., M. Laurenson, and L. Taylor (2001). "Diseases of humans and their domestic mammals: pathogen characteristics, host range and the risk of emergence". en. In: *Phil. Trans. R. Soc. Lond. B* 356.1411. Ed. by M. E. J. Woolhouse and C. Dye, pp. 991–999. DOI: `10.1098/rstb.2001.0889`.

Coghlan, J. P., J. S. Fan, B. A. Scoggins, and A. A. Shulkes (1977). "Measurement of extracellular fluid volume and blood volume in sheep". In: *Aust J Biol Sci.* 30.1-2, pp. 71–84.

Courtice, F. C. (1943). "The blood volume of normal animals". en. In: *The Journal of Physiology* 102.3, pp. 290–305. DOI: `10.1113/jphysiol.1943.sp004035`.

Daubney, R., J. R. Hudson, and P. C. Garnham (1931). "Enzootic hepatitis or rift valley fever. An undescribed virus disease of sheep cattle and man from east africa". en. In: *The Journal of Pathology and Bacteriology* 34.4, pp. 545–579. DOI: `10.1002/path.1700340418`.

18

El Mamy, A. B. O. et al. (2011). "Unexpected Rift Valley Fever Outbreak, Northern Mauritania". en. In: *Emerging Infectious Diseases* 17.10, pp. 1894–1896. DOI: `10.3201/eid1710.110397`.

Elliott, R. and F. Weber (2009). "Bunyaviruses and the Type I Interferon System". en. In: *Viruses* 1.3, pp. 1003–1021. DOI: `10.3390/v1031003`.

Fenton, A., D. G. Streicker, O. L. Petchey, and A. B. Pedersen (2015). "Are All Hosts Created Equal? Partitioning Host Species Contributions to Parasite Persistence in Multihost Communities". en. In: *The American Naturalist* 186.5, pp. 610–622. DOI: `10.1086/683173`.

Ferguson, N. M. et al. (2015). "Modeling the impact on virus transmission of *Wolbachia* -mediated blocking of dengue virus infection of *Aedes aegypti*". en. In: *Sci. Transl. Med.* 7.279, 279ra37–279ra37. DOI: `10.1126/scitranslmed.3010370`.

Fontaine, A., S. Lequime, I. Moltini-Conclois, D. Jiolle, I. Leparc-Goffart, R. C. Reiner, and L. Lambrechts (2018). "Epidemiological significance of dengue virus genetic variation in mosquito infection dynamics". en. In: *PLOS Pathogens* 14.7. Ed. by N. M. Ferguson, e1007187. DOI: `10.1371/journal.ppat.1007187`.

Gog, J. R., L. Pellis, J. L. Wood, A. R. McLean, N. Arinaminpathy, and J. O. Lloyd-Smith (2015). "Seven challenges in modeling pathogen dynamics within-host and across scales". en. In: *Epidemics* 10, pp. 45–48. DOI: `10.1016/j.epidem.2014.09.009`.

Golnar, A. J., M. J. Turell, A. D. LaBeaud, R. C. Kading, and G. L. Hamer (2014). "Predicting the Mosquito Species and Vertebrate Species Involved in the Theoretical Transmission of Rift Valley Fever Virus in the United States". en. In: *PLoS Neglected Tropical Diseases* 8.9. Ed. by C. M. Barker, e3163. DOI: `10.1371/journal.pntd.0003163`.

Hollingsworth, T. D., J. R. Pulliam, S. Funk, J. E. Truscott, V. Isham, and A. L. Lloyd (2015). "Seven challenges for modelling indirect transmission: Vector-borne diseases, macroparasites and neglected tropical diseases". en. In: *Epidemics* 10, pp. 16–20. DOI: `10.1016/j.epidem.2014.08.007`.

Iwami, S., B. P. Holder, C. A. Beauchemin, S. Morita, T. Tada, K. Sato, T. Igarashi, and T. Miura (2012). "Quantification system for the viral dynamics of a highly pathogenic simian/human immunodeficiency virus based on an in vitro experiment and a mathematical model". en. In: p. 12.

Jacobs, N. T., N. O. Onuoha, A. Antia, J. Steel, R. Antia, and A. C. Lowen (2019). "Incomplete influenza A virus genomes occur frequently but are readily complemented during localized viral spread". en. In: *Nature Communications* 10.1. DOI: `10.1038/s41467-019-11428-x`.

Kain, M. P. and B. M. Bolker (2019). "Predicting West Nile virus transmission in North American bird communities using phylogenetic mixed effects models and eBird citizen science data". en. In: *Parasites Vectors* 12.1, p. 395. DOI: `10.1186/s13071-019-3656-8`.

Koelle, K., A. P. Farrell, C. B. Brooke, and R. Ke (2019). "Within-host infectious disease models accommodating cellular coinfection, with an application to influenza†". en. In: *Virus Evolution* 5.2. DOI: `10.1093/ve/vez018`.

Kruschke, J. (2015). "Doing Bayesian Data Analysis: A tutorial with R and Bugs". en. In: *Doing Bayesian Data Analysis*. Elsevier, pp. i–ii. DOI: 10.1016/B978-0-12-405888-0.09999-2.

Krylova, O. and D. J. D. Earn (2013). "Effects of the infectious period distribution on predicted transitions in childhood disease dynamics". en. In: *Journal of The Royal Society Interface* 10.84, p. 20130098. DOI: 10.1098/rsif.2013.0098.

LaBeaud, A. D., J. W. Kazura, and C. H. King (2010). "Advances in Rift Valley fever research: insights for disease prevention:" en. In: *Current Opinion in Infectious Diseases* 23.5, pp. 403–408. DOI: 10.1097/QCO.0b013e32833c3da6.

Lequime, S., J.-S. Dehecq, S. Matheus, F. de Laval, L. Almeras, S. Briolant, and A. Fontaine (2020). "Modeling intra-mosquito dynamics of Zika virus and its dose-dependence confirms the low epidemic potential of Aedes albopictus". en. In: *PLOS Pathogens* 16.12. Ed. by E. A. McGraw, e1009068. DOI: 10.1371/journal.ppat.1009068.

Linthicum, K. J., S. C. Britch, and A. Anyamba (2016). "Rift Valley Fever: An Emerging Mosquito-Borne Disease". In: *Annual Review of Entomology* 61.1, pp. 395–415. DOI: 10.1146/annurev-ento-010715-023819.

Lloyd, A. L. (2001). "Realistic Distributions of Infectious Periods in Epidemic Models: Changing Patterns of Persistence and Dynamics". en. In: *Theoretical Population Biology* 60.1, pp. 59–71. DOI: 10.1006/tpbi.2001.1525.

Lloyd-Smith, J. O., S. Funk, A. R. McLean, S. Riley, and J. L. Wood (2015). "Nine challenges in modelling the emergence of novel pathogens". en. In: *Epidemics* 10, pp. 35–39. DOI: 10.1016/j.epidem.2014.09.002.

Mapder, T., S. Clifford, J. Aaskov, and K. Burrage (2019). "A population of bang-bang switches of defective interfering particles makes within-host dynamics of dengue virus controllable". en. In: *PLOS Computational Biology* 15.11. Ed. by J. A. Papin, e1006668. DOI: 10.1371/journal.pcbi.1006668.

Martin, L. B. et al. (2019). "Extreme Competence: Keystone Hosts of Infections". en. In: *Trends in Ecology & Evolution* 34.4, pp. 303–314. DOI: 10.1016/j.tree.2018.12.009.

Meegan, J. M. (1979). "The Rift Valley fever epizootic in Egypt 1977–1978 1. Description of the epizootic and virological studies". en. In: *Transactions of the Royal Society of Tropical Medicine and Hygiene* 73.6, pp. 618–623. DOI: 10.1016/0035-9203(79)90004-X.

Miao, H., X. Xia, A. S. Perelson, and H. Wu (2011). "On Identifiability of Nonlinear ODE Models and Applications in Viral Dynamics". en. In: *SIAM Review* 53.1, pp. 3–39. DOI: 10.1137/090757009.

Nanyingi, M. O., P. Munyua, S. G. Kiama, G. M. Muchemi, S. M. Thumbi, A. O. Bitek, B. Bett, R. M. Muriithi, and M. K. Njenga (2015). "A systematic review of Rift Valley Fever epidemiology 1931–2014". en. In: *Infection Ecology & Epidemiology* 5.1, p. 28024. DOI: 10.3402/iee.v5.28024.

Petrie, S. M., T. Guarnaccia, K. L. Laurie, A. C. Hurt, J. McVernon, and J. M. McCaw (2013). "Reducing Uncertainty in Within-Host Parameter Estimates of Influenza Infection by Measuring Both Infectious and

Total Viral Load". en. In: *PLoS ONE* 8.5. Ed. by J. D. Brown, e64098. DOI: 10.1371/journal.pone.0064098.

Petrie, S. M., J. Butler, I. G. Barr, J. McVernon, A. C. Hurt, and J. M. McCaw (2015). "Quantifying relative within-host replication fitness in influenza virus competition experiments". en. In: *Journal of Theoretical Biology* 382, pp. 259–271. DOI: 10.1016/j.jtbi.2015.07.003.

Pinilla, L. T., B. P. Holder, Y. Abed, G. Boivin, and C. A. A. Beauchemin (2012). "The H275Y Neuraminidase Mutation of the Pandemic A/H1N1 Influenza Virus Lengthens the Eclipse Phase and Reduces Viral Output of Infected Cells, Potentially Compromising Fitness in Ferrets". en. In: *Journal of Virology* 86.19, pp. 10651–10660. DOI: 10.1128/JVI.07244-11.

Quigley, J., J. Drewry, and K. Martin (1998). "Estimation of Plasma Volume in Holstein and Jersey Calves". en. In: *Journal of Dairy Science* 81.5, pp. 1308–1312. DOI: 10.3168/jds.S0022-0302(98)75693-0.

Roberts, G. O., A. Gelman, and W. R. Gilks (1997). "Weak convergence and optimal scaling of random walk Metropolis algorithms". en. In: *The Annals of Applied Probability* 7.1, pp. 110–120. DOI: 10.1214/aoap/1034625254.

Roche, B., M Eric Benbow, R. Merritt, R. Kimbirauskas, M. McIntosh, P. L. C. Small, H. Williamson, and J.-F. Guégan (2013). "Identifying the Achilles heel of multi-host pathogens: the concept of keystone 'host' species illustrated by *Mycobacterium ulcerans* transmission". en. In: *Environ. Res. Lett.* 8.4, p. 045009. DOI: 10.1088/1748-9326/8/4/045009.

Scharton, D., A. J. Van Wettere, K. W. Bailey, Z. Vest, J. B. Westover, V. Siddharthan, and B. B. Gowen (2015). "Rift Valley Fever Virus Infection in Golden Syrian Hamsters". en. In: *PLoS ONE* 10.1. Ed. by K. Kehn-Hall, e0116722. DOI: 10.1371/journal.pone.0116722.

Schulze-Horsel, J., M. Schulze, G. Agalaridis, Y. Genzel, and U. Reichl (2009). "Infection dynamics and virus-induced apoptosis in cell culture-based influenza vaccine production—Flow cytometry and mathematical modeling". en. In: *Vaccine* 27.20, pp. 2712–2722. DOI: 10.1016/j.vaccine.2009.02.027.

Simon, P. F., M.-A. de La Vega, E. Paradis, E. Mendoza, K. M. Coombs, D. Kobasa, and C. A. A. Beauchemin (2016). "Avian influenza viruses that cause highly virulent infections in humans exhibit distinct replicative properties in contrast to human H1N1 viruses". en. In: *Scientific Reports* 6.1. DOI: 10.1038/srep24154.

Smith, A. M., F. R. Adler, and A. S. Perelson (2010). "An accurate two-phase approximate solution to an acute viral infection model". en. In: *Journal of Mathematical Biology* 60.5, pp. 711–726. DOI: 10.1007/s00285-009-0281-8.

Somvanshi, P. R. and K. V. Venkatesh (2013). "Hill Equation". In: *Encyclopedia of Systems Biology*. Ed. by W. Dubitzky, O. Wolkenhauer, K.-H. Cho, and H. Yokota. New York, NY: Springer New York, pp. 892–895. DOI: 10.1007/978-1-4419-9863-7_946.

Svensson, A. (2007). "A note on generation times in epidemic models". en. In: *Mathematical Biosciences* 208.1, pp. 300–311. DOI: 10.1016/j.mbs.2006.10.010.

Taylor, L. H., S. M. Latham, and M. E. woolhouse (2001). "Risk factors for human disease emergence". en. In: *Phil. Trans. R. Soc. Lond. B* 356.1411. Ed. by M. E. J. Woolhouse and C. Dye, pp. 983–989. DOI: 10.1098/rstb.2001.0888.

Tesla, B., L. R. Demakovsky, H. S. Packiam, and E. A. Mordecai (2018). "Estimating the effects of variation in viremia on mosquito susceptibility, infectiousness, and R0 of Zika in Aedes aegypti". en. In: *PLOS Neglected Tropical Diseases* 12.8, p. 19.

Tuncer, N., H. Gulbudak, V. L. Cannataro, and M. Martcheva (2016). "Structural and Practical Identifiability Issues of Immuno-Epidemiological Vector–Host Models with Application to Rift Valley Fever". en. In: *Bulletin of Mathematical Biology* 78.9, pp. 1796–1827. DOI: 10.1007/s11538-016-0200-2.

Turell, M. J., D. J. Dohm, C. N. Mores, L. Terracina, D. L. Wallette, L. J. Hribar, J. E. Pecor, and J. A. Blow (2008). "Potential for North American Mosquitoes to Transmit Rift Valley Fever Virus [1]". en. In: *Journal of the American Mosquito Control Association* 24.4, pp. 502–507. DOI: 10.2987/08-5791.1.

Turell, M. J., W. C. Wilson, and K. E. Bennett (2010). "Potential for North American Mosquitoes (Diptera: Culicidae) to Transmit Rift Valley Fever Virus". en. In: *J Med Entomol* 47.5, pp. 884–889. DOI: 10.1093/jmedent/47.5.884.

Turell, M. J., S. C. Britch, R. L. Aldridge, D. L. Kline, C. Boohene, and K. J. Linthicum (2013). "Potential for Mosquitoes (Diptera: Culicidae) From Florida to Transmit Rift Valley Fever Virus". en. In: *J Med Entomol* 50.5, pp. 1111–1117. DOI: 10.1603/ME13049.

Turell, M. J., L. W. Cohnstaedt, and W. C. Wilson (2020). "Effect of Environmental Temperature on the Ability of *Culex tarsalis* and *Aedes taeniorhynchus* (Diptera: Culicidae) to Transmit Rift Valley Fever Virus". en. In: *Vector-Borne and Zoonotic Diseases* 20.6, pp. 454–460. DOI: 10.1089/vbz.2019.2554.

Vazquez-Prokopec, G. M., T. A. Perkins, L. A. Waller, A. L. Lloyd, R. C. Reiner, T. W. Scott, and U. Kitron (2016). "Coupled Heterogeneities and Their Impact on Parasite Transmission and Control". en. In: *Trends in Parasitology* 32.5, pp. 356–367. DOI: 10.1016/j.pt.2016.01.001.

Vloet, R. P. M., C. B. F. Vogels, C. J. M. Koenraadt, G. P. Pijlman, M. Eiden, J. L. Gonzales, L. J. M. van Keulen, P. J. Wichgers Schreur, and J. Kortekaas (2017). "Transmission of Rift Valley fever virus from European-breed lambs to Culex pipiens mosquitoes". en. In: *PLOS Neglected Tropical Diseases* 11.12. Ed. by M. J. Turell, e0006145. DOI: 10.1371/journal.pntd.0006145.

Wallinga, J and M Lipsitch (2007). "How generation intervals shape the relationship between growth rates and reproductive numbers". en. In: *Proc. R. Soc. B* 274.1609, pp. 599–604. DOI: 10.1098/rspb.2006.3754.

Weaver, S. C., N. L. Forrester, J. Liu, and N. Vasilakis (2021). "Population bottlenecks and founder effects: implications for mosquito-borne arboviral emergence". en. In: *Nat Rev Microbiol* 19.3, pp. 184–195. DOI: 10.1038/s41579-020-00482-8.

Webster, J. P., A. Borlase, and J. W. Rudge (2017). "Who acquires infection from whom and how? Disentangling multi-host and multi-mode transmission dynamics in the 'elimination' era". en. In: *Phil. Trans. R. Soc. B* 372.1719, p. 20160091. DOI: 10.1098/rstb.2016.0091.

Wichgers Schreur, P. J. et al. (2020a). "Safety and efficacy of four-segmented Rift Valley fever virus in young sheep, goats and cattle". en. In: *npj Vaccines* 5.1. DOI: 10.1038/s41541-020-00212-4.

— (2020b). "Safety and efficacy of four-segmented Rift Valley fever virus in young sheep, goats and cattle". en. In: *npj Vaccines* 5.1. DOI: 10.1038/s41541-020-00212-4.

Wichgers Schreur, P. J., R. P. M. Vloet, J. Kant, L. van Keulen, J. L. Gonzales, T. M. Visser, C. J. M. Koenraadt, C. B. F. Vogels, and J. Kortekaas (2021). "Reproducing the Rift Valley fever virus mosquito-lamb-mosquito transmission cycle". en. In: *Sci Rep* 11.1, p. 1477. DOI: 10.1038/s41598-020-79267-1.

Yan, A. W., J. Zhou, C. A. Beauchemin, C. A. Russell, W. S. Barclay, and S. Riley (2020). "Quantifying mechanistic traits of influenza viral dynamics using in vitro data". en. In: *Epidemics* 33, p. 100406. DOI: 10.1016/j.epidem.2020.100406.